

DEVELOPMENT OF A (NEW) DIGITAL COLLIMATOR

*W. Schauerte and N. Casott
University of Bonn, Germany*

1. INTRODUCTION

Nowadays a modern measuring technique requires testing methods which have a high automation standard and work as far as possible in an objective manner. Getting more objectivity means that the intrinsic measuring process doesn't depend on the technical skill of an observer (tired, well rested) but exclusively on the quality of the testing assembly in connection with the integrated data analysis. The efforts in eliminating man out of the measuring procedure mainly rely upon his subjectivity and others failings like cutting the data flow.

The presented development is the second step of a precise measuring system which avoids the disadvantage of visually working methods by conventional collimator systems. Therefore an older ASKANIA-Collimator ($f = 550$ mm) was modified. On one hand the focal length was magnified on an equivalent length of about 2750 mm in adding an optical element and on the other hand in replacing a linear image PCD-Sensor instead of the normally used reticule. Using this hardware [5] a new evaluation software is implemented. The hardware and software components are pursuing the following:

1. Designing an automatic measuring process, which integrates the recording and analysis procedure.
2. The attainable accuracy of this prototype should be $< 0.3''$.
3. The application of intensity-based image matching, with applied cross-correlation techniques is used to get a better sub-pixel resolution.

2. REALIZED MEASURING CONCEPT

2.1 Hardware configuration

The first presentation of the new collimator measurement system [1] gives a good overview over the different system components and its disposition. In the meantime the hardware configuration has changed in several components. To make the measure faster a 12 Bit AD-converter as a PC-card was implement into the computer (see Fig 1). It allows a voltage resolution of about 1 mV based on a 2.5 til 5.0 voltage level against 5 mV in the configuration before. Therefore some effects appear which couldn't be "seen" in consequence of the lower resolution.

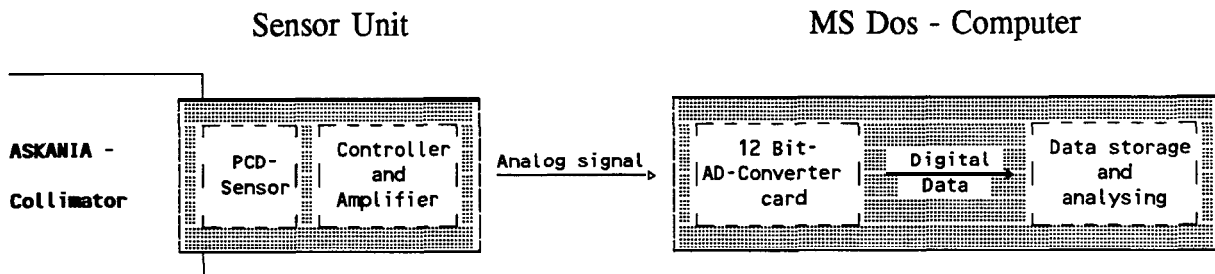


Fig. 1 Block diagram of the collimator measuring system

2.2 Influences of signal falsifications

In the following explanations the effects are presented with the most important falsifications on the sensor signal. It was a hard work to detect and to classify each one with the signal which has been transmitted.

Computer Interrupts

The signal falsifications of Fig. 2 show some upside-down which are caused by the computer sending several interrupts (e.g. keyboard interrupt in different time rates (4 Hz, 33 Hz, etc.)). They depend on the internal control system of the computer. So the control system allocates the CPU a higher priority than an introduction of a program code.

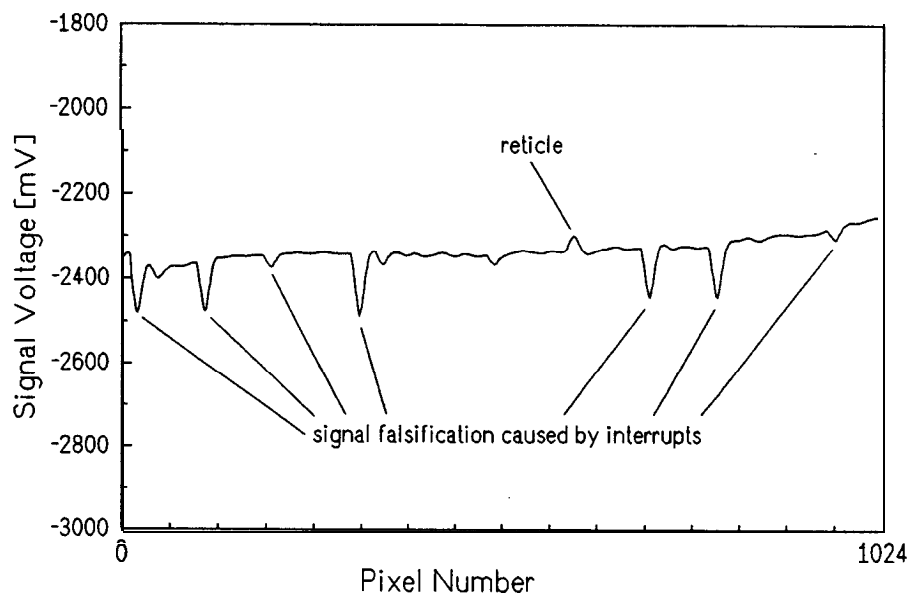


Fig. 2 Sensor signal when the interrupts are unlocked

That means if the CPU gets an interrupt during the signal output of the sensor the program will be stopped as long as the interrupt works. This causes delays in the time rate. If a delay appears a pixel element gets more integration time to collect light and shows a higher voltage value. In our case it is a higher negative voltage value.

This problem can be avoided, if the interrupts are frozen before an output process starts [6]. Therefore the special assembler introduction CLI (Code: FA) has to be included into a program line. After finishing the output process all interrupts have to be released with the assembler introduction STI (Code: FB). Doesn't that happen, the computer is put out of order and the hardware must be reset. If the interrupts are blocked correctly the sensor signal doesn't show the typical falsification of Fig. 2.

Shielding the video signal transmission and the sensor itself

If you make experiments with sensitive sensors in many cases the signal will be measured as a mV-measure. Then it is necessary shielding e.g. the junction cable for the video-signal transmission and the sensor itself. Another influence is the interference frequency of the 220V net for the power supply of the cold light source.

'Finger-print' of the image sensor

It is evident that each photodiode has its own characteristic of sensitiveness because its darkcurrent and the gradient of its characteristic line vary in a more or less band width. Investigations of our image sensor show typical characteristics (finger-prints) depending on the integration time and its signal strength (see Fig. 3).

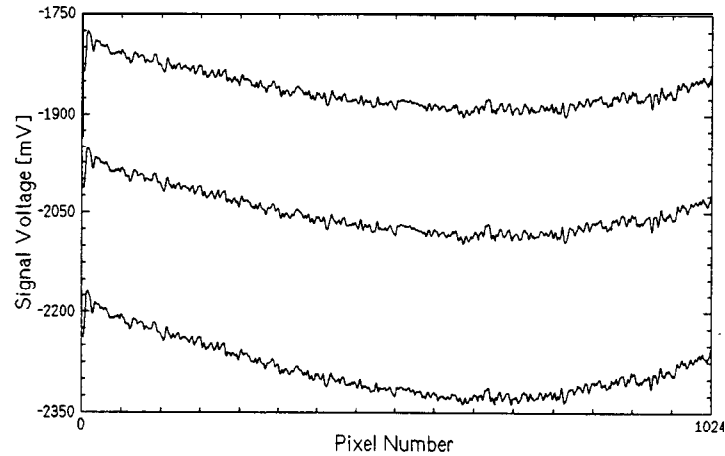


Fig. 3 Finger-prints of the image sensor

The requirement of this procedure may be documented by Fig. 4 and 5. Figure 4 shows the sensor signal (incl. reticule image) without any correction, meanwhile Fig. 5 describes the corrected signal, which has been transformed into a good conditioned measuring signal. Therefore several correction values are determined for each pixel correcting the transmitted value.

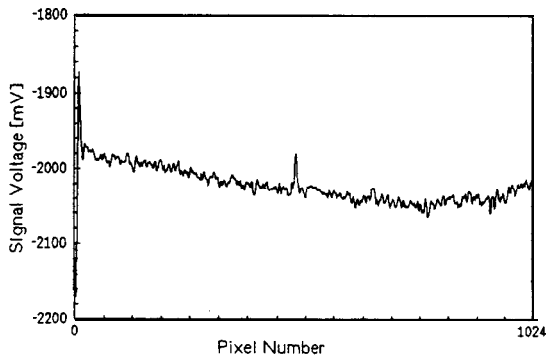


Fig. 4 Transmitted sensor signal without finger-print correction

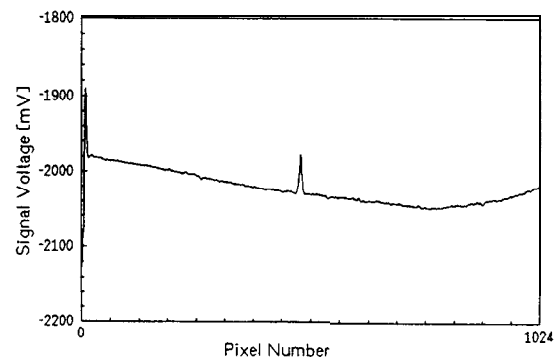


Fig. 5 Corrected sensor signal

Determination of the focal length

In most high precision measurements a system calibration has to be done. This procedure leads to the equivalent focal length. The corresponding standard deviation gives a good impression whether remaining errors influence the system quality, additionally. The calibration function (observation equation) has to be a linear function. The general observation equation has been derived from Casott [1, see Eq. (5.4)] or [5, see Eq. (2)] as:

$$\alpha_i = \frac{u_i \cdot 0.025 \text{ mm}}{f_E [\text{mm}]} \cdot \rho \quad (1)$$

with 0.025 mm = pixel pitch,
 f_E = equivalent focal length of about ≈ 2750 mm,
 u_i = estimated shift of the reticule line [number of pixels].

Differences from the linearity are caused from the optical element which was built in, additionally. Therefore the used working range has to be limited. With the values written above let the scale function be for a range of about ± 0.07 gon:

$$\alpha_i = u_i \cdot 0.000579 [\text{gon}] = u_i \cdot 0.579 [\text{mgon}] \quad (2)$$

Equation (2) leads to a system resolution of about 0.58 mgon, when a shift of one pixel pitch may be detected. If a higher resolution is taken into account, special procedures of estimating are necessary described in the following section.

3. INTENSITY-BASED MATCHING WITH APPLIED CROSS-CORRELATION TECHNIQUES

3.1 Preliminary remarks

Normally image matching starts from two or more digital or digitized images. Assume that the first measurement contains for example the position of the horizontal reticule mark (r') than its position (r'') varies in connection with a position shifting given in each additional measurement. This can be related by

$$(r') = T_G(r''; p_G) \quad (3)$$

where T_G is a specified geometric linear-mapping function reflecting the knowledge about the geometric relationship between the images, and p_G is a set of unknown parameters [4]. FÖRSTNER [2] describes the intensity on one image (g') related on the other (g'') by

$$g' = T_I(g''; p_I) \quad (4)$$

where the intensity-mapping function T_I contains the knowledge about the intensity relation between the images, again with the vector p_I being unknown. Both equations lead to the complete model of image matching

$$g'(r') = T_I\{g''[T_G(r''; p_G)]; p_I\} \quad (5)$$

The mapping functions T_G and T_I may be deterministic, stochastic, and/or piecewise continuous [4, p. 292].

It is very important for the solution of the problem to find or to find not the corresponding signal structure of the reticule mark in all images. That means the signal function of the reticule is relevant to an object location procedure. The model equation can then be written as

$$g(x) = T_I\{f[T_G(y; p_G)]; p_I\} + n(x) \quad (6)$$

where g' , g'' , r' , and r'' have been replaced for a one-dimensional signals by g , f , x , and y , respectively, and the observational noise component $n(x)$ is stated explicitly [4, p. 298]. The

problem will be reduced in doing a similarity measure how well the two ore more images match. This is usually based on the normalized cross-correlation or on a function of intensity differences of the values themselves (e.g. sum of squared differences or sum of absolute differences), actually measuring the shift or distance between the images.

3.2 Cross-correlation technique for one-dimensional signals

Picking out the cross-correlation technique is based on two assumptions [2] :

1. The two corresponding image sections geometrically differ only due to a shift (translation).
2. The two images radiometrically differ only due to brightness and contrast.

When the one-dimensional case is treated, the model reads as

$$g_1(x_i) = f(x_i) + n_1(x_i) \tag{7}$$

$$g_2(x_i) = g_1(x_i - u) + \bar{n}(x_i) \tag{8}$$

with

$$\bar{n}(x_i) = n_2(x_i) - n_1(x_i) \tag{9}$$

The principle of estimating u is to search for the maximal correlation coefficient ρ_{12} of g_1 and g_2 [4, p. 317]:

$$\rho_{12}(u) = \max \frac{\text{Cov}[g_1(x_i - u), g_2(x_i)]}{\sqrt{V[g_1(x_i - u)] \cdot V[g_2(x_i)]}} = \frac{\sigma_{g_1 g_2}(u)}{\sigma_{g_1}(u) \cdot \sigma_{g_2}} \rightarrow \hat{u} \tag{10}$$

with

$$\sigma_{g_1 g_2}^2(u) = \frac{1}{m-1} \cdot \left[\sum_{i=1}^m g_1(x_i - u) \cdot g_2(x_i) - \frac{1}{m} \cdot \sum_{i=1}^m g_1(x_i - u) \cdot \sum_{i=1}^m g_2(x_i) \right], \tag{11}$$

$$\sigma_{g_1}^2(u) = \frac{1}{m-1} \cdot \left[\sum_{i=1}^m g_1^2(x_i - u) - \frac{1}{m} \cdot \left(\sum_{i=1}^m g_1(x_i - u) \right)^2 \right], \tag{12}$$

$$\sigma_{g_2}^2 = \frac{1}{m-1} \cdot \left[\sum_{i=1}^m g_2^2(x_i) - \frac{1}{m} \cdot \left(\sum_{i=1}^m g_2(x_i) \right)^2 \right]. \tag{13}$$

As the estimates of the empirical mean and variances are taken into account, differences in brightness and contrast are immediately compensated for. This fact was very important to take a decision to this method. The estimation process usually exists as an iterative type of search starting from an approximation value for the shift, stopping in case a relative maximum of ρ_{12} is found. In general it leads to an integer pixel position. You will find that the rounding error is too dominant. Therefore an interpolation of the correlation function is useful, what Fig. 6 shows. The integer position of the maximum of $\rho(u)$ specifies u_0 and the two neighboring positions u_- and u_+ with its corresponding values ρ_0, ρ_- and ρ_+ . A quadratic

interpolation of $\rho(\mathbf{u})$ leads to the estimated shift

$$\hat{u} = u_0 - \frac{\rho_+ - \rho_-}{2(\rho_+ - 2\rho_0 + \rho_-)} \cdot \Delta x \tag{14}$$

and the expression for the corresponding variance

$$\sigma_u^2 = \frac{1}{m} \cdot \frac{1 - \rho_0}{\rho_0} \cdot \frac{\Delta x^2}{-\rho_+ + 2\rho_0 - \rho_-} \tag{15}$$

where Δx is the spacing between the u_i in both formulas. The maximum achievable correlation coefficient is limited by the signal-to-noise ratio which shows its influence in the quotient of the second term of formula (15).

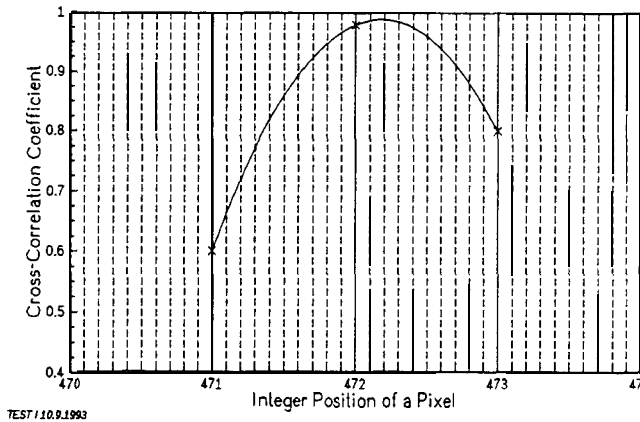


Fig. 6 Quadratic interpolation method

Figure 6 shows the situation described before. The values of the correlation coefficients e.g. 0.6, 0.98 and 0.8 illustrate that the maximum correlation would not coincide with an integer pixel number. Let a tenth pixel resolution be possible the estimated reticule position is 472.2.

3.3 Realization of the measure procedure in practice

The following statements assume that we determine measurements between the reticule position of the first registered signal image (reference position) related to each other signal images we get after varying the orientation of the collimation axis. Putting into practice the operator in connection with the developed software different steps have to be performed:

1. Let the illumination of the sensor elements be in band width between 1.0 and 2.3 V, otherwise the quality of the signal-to-noise ratio impairs the signal evaluation systematically.
2. The analog data of the sensor signal will be transmitted into the computer passing the A-/D-converter card. The integration time lasts about 1.1 s (nearly) eliminating e.g. the remaining errors of 50 Hz frequency (220 V net) and the effects in connection with the sensor circuit. Another correction is the “finger-print” of the sensor (Section 2.).
3. A simple way to find an approximation (integer) value of the reticule position on the sensor can be the first derivative of the sensor signal (Fig. 7). Then searching the maximum and minimum values of the new function at the positions u_{\max} and u_{\min} , respectively. A special program routine examines that both values are placed

in a small window varying with the line width of the reticule. The mean

$$\bar{u} = \frac{1}{2} (u_{\max} + u_{\min})$$

is calculated as an integer number.

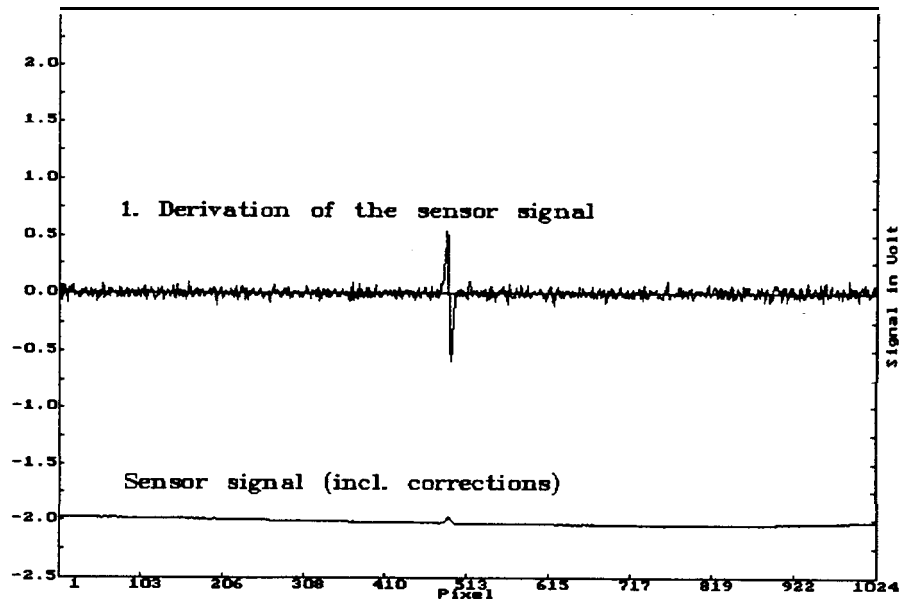


Fig. 7: Hardcopy of the PC-Monitor

4. It is very helpful to define a window in connection with first signal analysis before the correlation calculation starts. This procedure reduces the number of multiplications and the influences of remaining errors in the signal structure if besides the reticule signal there will be any white noise. The window size was fixed as an integer number $\pm 4 \cdot (\bar{u} - u_{\max})$ neighboring the position \bar{u} .
5. If a new measurement is executed then the steps 2 and 3 (step 4 has to perform only for one time) are repeated.
6. The cross-correlation process starts and leads to the estimated shift between the two image signals.
7. Repeating the steps 5 til 6; etc.

In connection with the calibration steps (shown in Section 2) and the new software first test measurements promise an accuracy of about 0.2”.

4. CONCLUSION

An opto-electronic collimator measurement system was described, which allows non visual measurements in contrast to the conventional methods used nowadays in most of the geodetic test laboratories. Therefore a linear image PCD-Sensor is adapted in the focal plane of a modified 550mm-ASKANIA-Collimator. In connection with a 12bit AD-PCcard the analog signals of the sensor are converted into digital signals. To evaluate a signal correctly it is necessary to know all influences which cause a significant falsification. Several examples are given. The approximate reticule position is detected with a simple evaluation method (first derivative of the signal). Following this step the variation of the signal position in a measuring process is calculated very precisely with the cross-correlation technique.

A significant enhancement in respect to the 0.2" will be expected if the other ASKANIA-Collimator (nominal focal length $f = 2250$ mm) has been correspondingly modified. Another possibility in improving the system accuracy is to take linear or area image sensors with smaller pixel sizes. In connection with these improvements an accuracy of less or equal than 0.05" will be realizable, which is necessary to investigate e.g. the influence of the magnetic fields on compensators of automatic levels and theodolites.

REFERENCES

- [1] N. Casott, Entwicklung eines Programmsystems zur Steuerung des automatisierten Meßablaufs eines Digitalkollimators mit integrierter Signalanalyse, unveröff. Diplomarbeit, Bonn 1993
- [2] W. Förstner, Image Matching and Surface Reconstruction, Internal Paper 1992
- [3] Hamamatsu, Technical Data Sheet of the PCD Linear Image Sensors Type S2304, July 1985
- [4] R. M. Haralick and L. G. Shapiro (eds.), Computer and Robot Vision, Addison-Wesley Publishing Company, New York 1993
- [5] W. Schauerte, Einsatz von CCD-/PCD-Technologien im Prüfaborbereich, Contributed paper to the 6th International FIG-Symposium on Deformation Measurements, 24-28 February 1992, Hannover, Germany
- [6] P. Wollschlaeger, PC Intern, Teil 2., Computer Persönlich, Ausgabe vom 11.10.1989